13th World Conference on Earthquake Engineering
Vancouver, B.C., Canada
August 1-6, 2004
Paper No. 794

ANALYSIS ON ELASTO-PLASTIC BEHAVIOR OF AN EXISTING REINFORCED CONCRETE BUILDING RETROFITTED BY STEEL-FRAMED BRACES IN DIFFERENT ARRANGEMENTS AND SIMPLIFIED EVALUATION METHOD OF HORIZONTAL BEARING CAPACITY OF THE RETROFITTED BUILDING

Tatusya KOMURO[1] and Masaya HIROSAWA[2]

SUMMARY

Using analysis models of a building retrofitted with steel-framed braces, this study analyzes the effects of different brace arrangements on the elasto-plastic behavior of the retrofitted building and the states of stress in the members in the retrofit zones to determine the characteristics of elasto-plastic behavior achieved with different bracing arrangements. Then, on the basis of the effects of different bracing arrangements determined, the study proposes a seismic retrofit design method. The results and findings of this study can be summarized as follows:

1) A retrofit design calculation method and conditions for applying the method have been proposed, and usefulness and practicality of the method have been confirmed.
2) Increasing the horizontal load-carrying capacity of the upper stories is difficult in the case of multi-story continuous bracing, while in the case of discontinuous bracing; the load-carrying capacity increases in proportion to the number of braces. Discontinuous bracing also makes it easy to achieve the required stiffness of each story and can be used as an effective means of reducing the earthquake response of a building.
3) Retrofit design using discontinuous bracing depends on yielding of braces and requires confirming the safety of adjoining members (e.g., lower-story columns, adjoining beams).
4) In cases where discontinuous bracing is used, it is desirable that braces be arranged more or less regularly, such as in a checkered pattern.

INTRODUCTION

A common practice in seismic retrofit design in Japan today is to use multi-story continuous bracing using steel-framed braces because it is an effective seismic retrofit method for increasing strength and achieving high ductility. Multi-story continuous bracing used in middle- or high-rise buildings, however, may make it difficult to achieve the required stiffness under earthquake loading if a very large number of braces are

[1]Graduate student, Kogakuin University, Tokyo, Japan. Email: BQB03635@nifty.ne.jp
[2]Professor, Kogakuin University, Tokyo, Japan. Email: dt10760@ccs.kogakuin.ac.jp

used. In order to make effective use of bracing, therefore, it is necessary to develop a seismic retrofit method that enables achieving the required strength and stiffness at each floor level by distributing braces in a discontinuous manner.

Dr. Sukenobu TANI and others [1, 2] conducted model tests using steel tendons to investigate the effects of different bracing arrangements and concluded that the lateral load carrying ratio achieved by discontinuous bracing is higher than that achieved by multi-story continuous bracing, and that discontinuous bracing effectively reduces axial forces acting on columns so as to reduce factors contributing to flexural deformation. Dr. Yasutoshi SONOBE and others [3] conducted a study on steel-framed reinforced concrete structures with shear walls arranged in a checkered pattern and reported that a structural frame reinforced with shear walls arranged in a checkered pattern acted integrally to resist external forces until the maximum load-carrying capacity was reached or nearly reached. Very few studies, however, have been undertaken on subjects like these, and only a limited number of studies have dealt with the relative merits of different arrangements of structural members. The number of structures that have been built with structural members arranged in a discontinuous manner is also small.

This paper analyzes the effects of different arrangements of strengthening members (braces) on the seismic performance of a retrofitted building, proposes a design method including the use of discontinuous arrangement of principal strengthening members in the seismic retrofit design of existing buildings, and describes conditions for applying the method.

OUTLINE OF ANALYSIS MODELS

The building used, as the analysis model is a school building completed in 1980, and part of the building was modeled for the purposes of analysis. Figure 1 is a column–beam plan, and Figure 2 is a framing elevation along line Y1. Table 1 a) and b) show the column and beam sections, and Table 2 shows the strength of the materials used. In the analysis, the plane of structure along line Y1 was modeled as a plane frame, and an incremental loading static elasto-plastic analysis was conducted. The computer program used for the analysis is Dr. Kangning LI's CANNY.

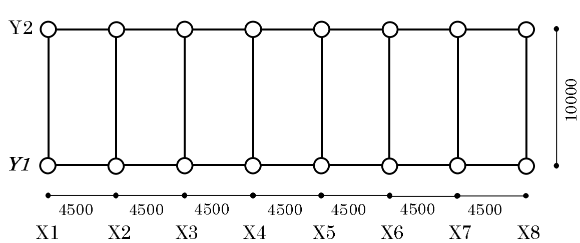

Figure 1 Column-Girder Plan (unit: mm)

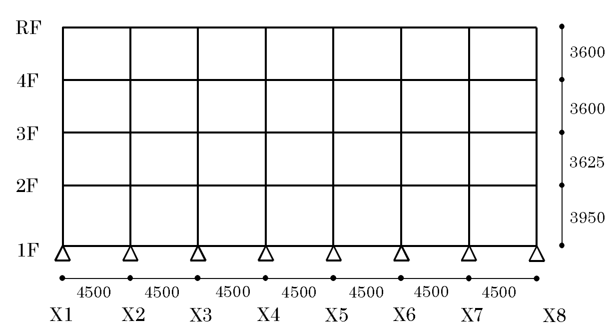

Figure 2 Framing Elevation (unit: mm) (Case1)

In the modeling, beams and columns are replaced with linear elements that have rigid zones at both ends, bending springs at member ends, and shear springs and axial springs at midpoints; diagonal members of steel-framed braces are replaced with axial springs; and the foundation is replaced with vertical springs. Bending, shear and axial deformation are taken into account for the beams and columns; axial deformation is taken into account for steel-framed braces; and compressive deformation and tensile deformation are taken into account for the foundation. Beam–column connections are assumed to be rigid.

Table 1 a) Schedule of Column Sections

Floor	3rd, 4th	1st, 2nd
Section	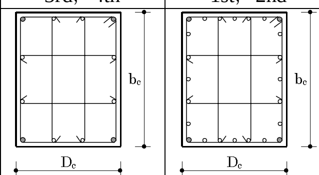	
(width : b_c)×(depth : D_c)	$900_{mm}\times700_{mm}$	$900_{mm}\times700_{mm}$
Main	4-D32, 8-D25	4-D32, 18-D25
Hoop	4-D10-100@	4-D13-100@

Table 1 b) Schedule of Guarder Sections

Floor		Both Ends	Center
RF	Section	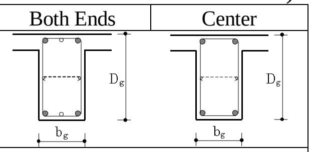	
	$b_g\times D_g$	$350_{mm}\times650_{mm}$	
	Top	2-D32, 1-D25	2-D32
	Bottom	2-D32, 1-D25	2-D32
	Stirrup	2-D13-200@	
4F	Section	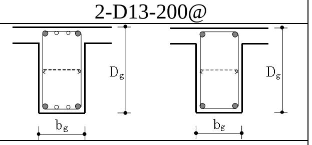	
	$b_g\times D_g$	$350_{mm}\times650_{mm}$	
	Top	2-D32, 2-D25	2-D32
	Bottom	2-D32, 2-D25	2-D32
	Stirrup	2-D13-100@	
3F	Section	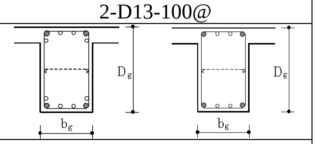	
	$b_g\times D_g$	$400_{mm}\times650_{mm}$	
	Top	2-D32, 4-D25	2-D32, 2-D25
	Bottom	2-D32, 4-D25	2-D32, 2-D25
	Stirrup	2-D13-100@	

Floor		Both Ends	Center
2F	Section	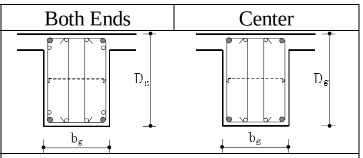	
	$b_g\times D_g$	$500_{mm}\times700_{mm}$	
	Top	2-D32, 4-D25	2-D32, 2-D25
	Bottom	2-D32, 4-D25	2-D32, 2-D25
	Stirrup	4-D13-100@	
1F	Section	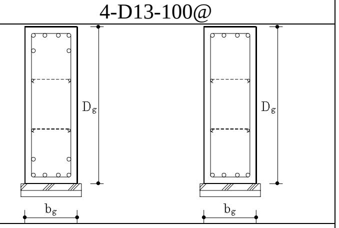	
	$b_g\times D_g$	$400_{mm}\times1200_{mm}$	
	Top	6-D22	4-D22
	Bottom	6-D22	4-D22
	Stirrup	2-D10-150@	

note:
1. Auxiliary axial reinforcement in web is D10.
2. D10, D13, D25 and D32 are the deformed bars of section area 71.3, 127, 507 and 794mm^2.
3. ??@ etc. expresses the interval of a shear reinforcement.

Table 2 Material Used

Concrete	Normal concrete : F_c=21 N/mm^2, E_c=2.12×10^4 N/mm^2
Reinforcing	Main: SD345 (400 N/mm^2) Share: SD295 (350 N/mm^2)
Pile foundation	Five PC pile, Diameter: 350 φ, Length: 35.0m, Vertical spring strength*1 (Crush (5741.6 kN), Uplift (1510.2 kN)) Vertical spring stiffness *1 (656.79kN/mm)
Steel brace	1st , 2nd Floor: SN400 (F=258.9 N/mm^2), H-200×200×8×12 3rd , 4th Floor: SN400 (F=258.9 N/mm^2), H-175×175×7.5×11

note:*1. Strength and Stiffness with five prestressed concrete pile

Table 3 Distribution of External Lode

Floor	P
RF	2.345
4F	1.583
3F	1.268
2F	1.000

Restoring force characteristics are modeled as trilinear restoring force characteristics with a cracking point and a yield point. However, the axial springs of the columns and beams, the axial springs for steel-framed braces, and the vertical springs of the foundation are modeled as bilinear restoring force characteristics.

The flexural cracking strength values for the beams and columns were taken from Reference 4; the ultimate flexural strength values from Reference 5; the shear cracking strength and ultimate strength values for the beams from Reference 5; the shear cracking strength values for the columns from Reference 6; the ultimate shear strength values from Reference 5; and the stiffness reduction ratios at the failure of the beams and columns from Reference 6. The compression capacity and tension capacity of steel-framed braces are determined in accordance with Reference 7. The compression capacity and pull-out capacity of the foundation are determined in accordance with Reference 8, and the vertical spring stiffness is determined in accordance with Reference 9.

Post-peak strength reduction of the members that fail by shear failure is not taken into account. Story shear distribution [4] based on the Japanese seismic design standard provisions determined for the entire structure analyzed is taken as the external force distribution. External forces were distributed among different stories according to the floor area governed by each node at the story level under consideration. The external force distribution is shown in Table 3.

Type of the analyzed building

The steel-framed braces used to strengthen the building were modeled as X-shaped diagonals. Ignoring the steel frames and assuming that column–frame connections and beam–frame connections (strengthening member connections) are free from failure; the frame designs shown in Figure 3 were analyzed. The same number (seven locations) of braces was used for all frame configurations. Case 1 is the pre-retrofit pure frame structure; Case 2, a frame with multi-story continuous bracing; Case 3, a frame with mountain-shaped bracing; Case 4, a structure with discontinuous bracing; and Case 5, a structure with checkered bracing.

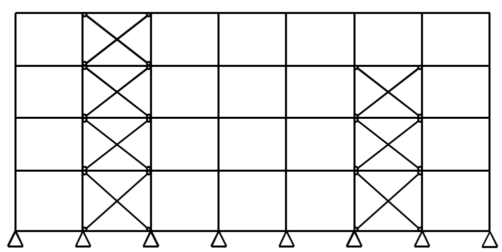

a) Case 2 (Multi-Story)

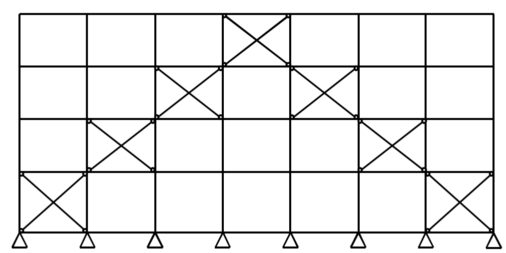

b) Case 3 (Mountain Type)

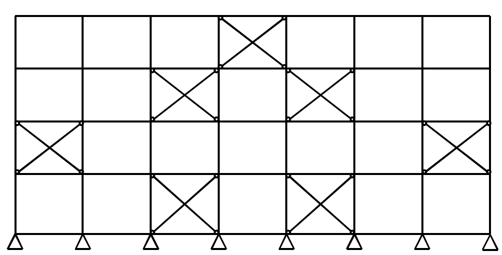

c) Case 4 (Discontinuous)

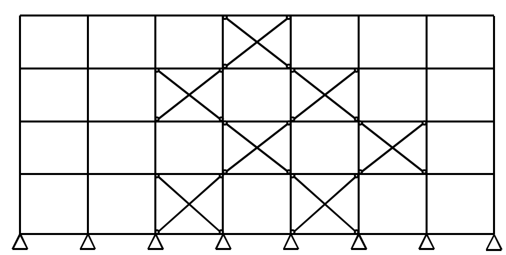

d) Case 5 (Checkered Type)

Figure 3 The Analysis Frame Models of Each Case

RESULTS AND DISCUSSION

Relationship between story shear force *Q* and story drift angle *R*

Figure 4 a) to e) show the analytically derived relationships between story shear force and story drift angle *R* for each case. The broken lines and numbers indicate the overall story drift angle *Ra*. Figure 5 a) shows changes in story shear force at the first floor level, and Figure 5 b) compares story shear forces at the first floor level. These figures indicate the following:

1) In Case 1 (pre-retrofit case; pure frame), the deformation of the lowest 2^{nd} story tends to be large, while in Case 2 (multi-story) similar deformation occurs at all story levels. In Cases 3, 4 and 5, deformation similar to the deformation in the case of multi-story continuous bracing occurs until the story drift angle reaches *R*=1/400 or so, but greater deformation occurs at the lowest 2^{nd} story at story drift angles of *R*=1/200 and *R*=1/100.
2) Comparison of pre-retrofit and post-retrofit story shear forces at the first story level shows that when the story drift angle is *R*=1/100, story shear force in Case 2 (multi-story), Case 3 (mountain), Case 4 (discontinuous) and Case 5 (checkered) increases by 62%, 91%, 91% and 95%, respectively. Thus, the load-carrying capacity increases in all cases, but the percentage of increase in load-carrying capacity in Case 2 (multi-story continuous) is slightly lower than in the other cases. Similar tendencies are indicated for the second to forth stories.
3) Stiffness is slightly lower in Case 4 (discontinuous) than in Case 3 (mountain) and Case 5 (checkered). This is because of rapid progress of yielding of braces and adjoining members. In Case 2 (multi-story), in which this tendency is particularly strong, stiffness is low largely because the rotation of the pile foundation underlying the multi-story bracing is predominant.
4) In all cases, story shear forces at overall rotation angles of *R*=1/200 and *R*=1/100 are 0.85–0.93 and 0.97–0.99 times the story shear forces at *R*=1/50, indicating that the load-carrying capacity of the frame is reached or nearly reached at *R*=1/200.

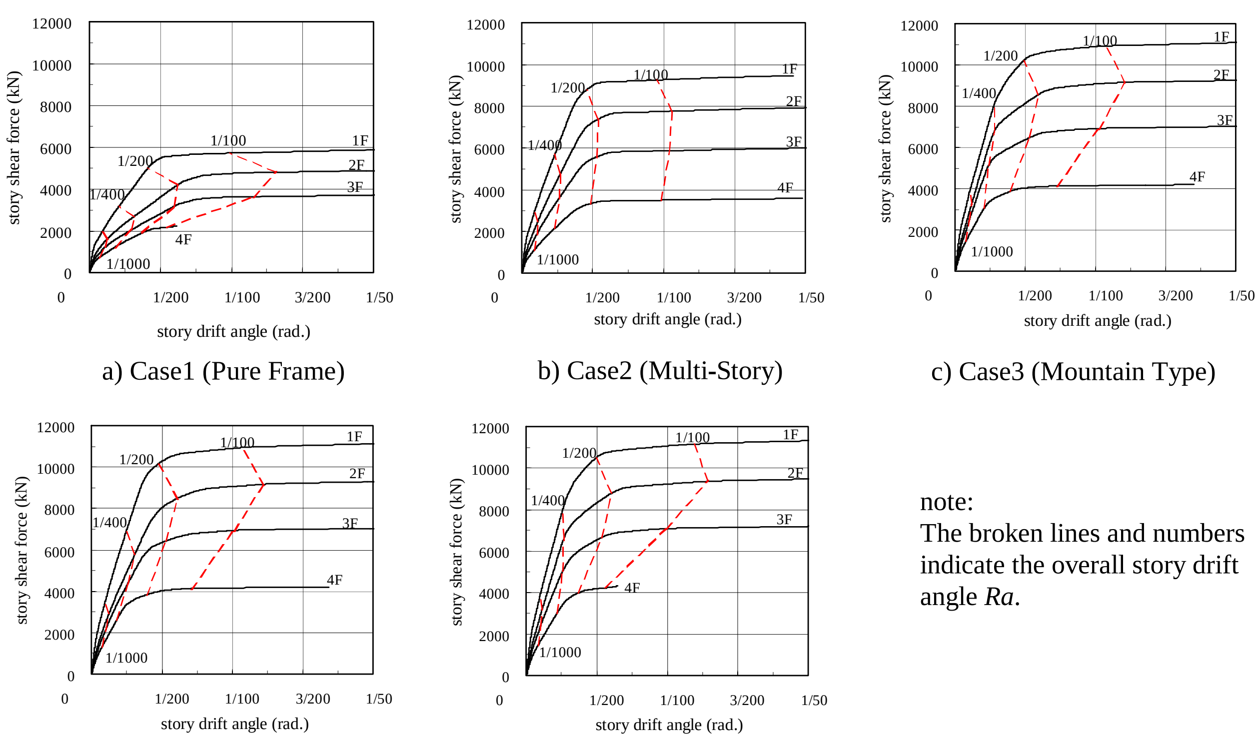

a) Case1 (Pure Frame)

b) Case2 (Multi-Story)

c) Case3 (Mountain Type)

d) Case4 (Discontinuous)

e) Case5 (Checkered Type)

note:
The broken lines and numbers indicate the overall story drift angle *Ra*.

Figure 4 Story Shear Force *Q* vs. Story Drift Angle *R*

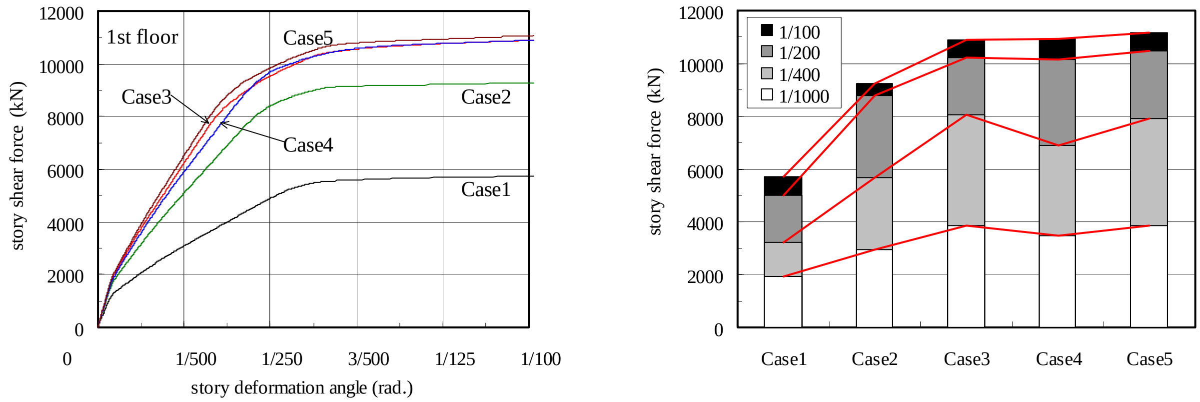

a) Story Shear Force Q vs. Story Drift Angle R at the 1st Floor

b) Story shear force Q at the 1st Floor

Figure 5 Changes and Compares Story Shear Force Q at the 1st Floor

Mode of failure

Figure 6 shows the occurrence of yield hinges at overall story drift angles *Ra* of 1/200 and 1/100. In the figure, different symbols for yield hinges correspond to different ranges of the ductility factor determined by dividing the response displacement at each step by the displacement of each member when its load-bearing capacity is reached. Figure 6 indicates the following:

1) Examination of the states of yielding at *R*=1/200 reveals that in Case 1 (pure frame), flexural yielding of beams occurred only at a small number of locations, and the story shear force in this case was 0.85% of the story shear force at *R*=1/50. The collapse mechanism was largely formed at *R*=1/100, but there was as yet no yield hinge at the fourth floor level.
2) In Case 2 (multi-story continuous), a rotational mode of failure occurred because of the pull-out of the foundation at the lower end of the multi-story bracing, accompanied by bending and shear failure of adjoining beams. In Cases 3, 4 and 5, in which braces were arranged in a discontinuous manner, yielding of the braces occurred first, and almost all braces failed in tension or compression at *R*=1/200.
3) In all retrofit cases (Case 2 to Case 5), pull-out of the pile foundation occurred. In the multi-story continuous bracing case, considerable pull-out force and compressive force occurred at the lower end of the multi-story bracing (Case 2, X2). In the discontinuous bracing cases, large pull-out forces and compressive forces occurred at the base of the outermost span (Case 3, X1; Case 4, X1; Case 5, X3).

Shear force acting on braced frame

The ratio between the sum of shear forces Q_y occurring at the failure of the braces in a braced frame (braces and columns at both sides) and the working shear force Q was defined as RQ ($=Q/Q_y$). Figure 7 compares RQ values corresponding to different modes of deformation, calculated from the average values of Q_y and Q of the first-floor brace frames. The Q_y values are shown in Table 4. Figure 7 indicates the following:

1) In Case 2 (multi-story), RQ was slightly lower than 0.9 at *R*=1/200. In this case, RQ at the fourth floor level was slightly lower than 0.50, though not shown in the figure. Thus, the amount of shear force to be resisted by the braced frames at the highest floor level was small.
2) In Cases 3, 4 and 5, RQ values ranged from 1.0 to 1.1 at *R*=1/200, indicating that the load-carrying capacity of the braced frames was reached or nearly reached at all floor levels.
3) The RQ distributions in Case 3 (mountain) and Case 5 (checkered) do not show significant differences. In Case 4 (discontinuous), the rate of increase in RQ tends to be somewhat lower. Since, however, the RQ values are larger than those in Case 2 (multi-story), it can be said that discontinuous bracing is more effective in increasing strength than multi-story continuous bracing.

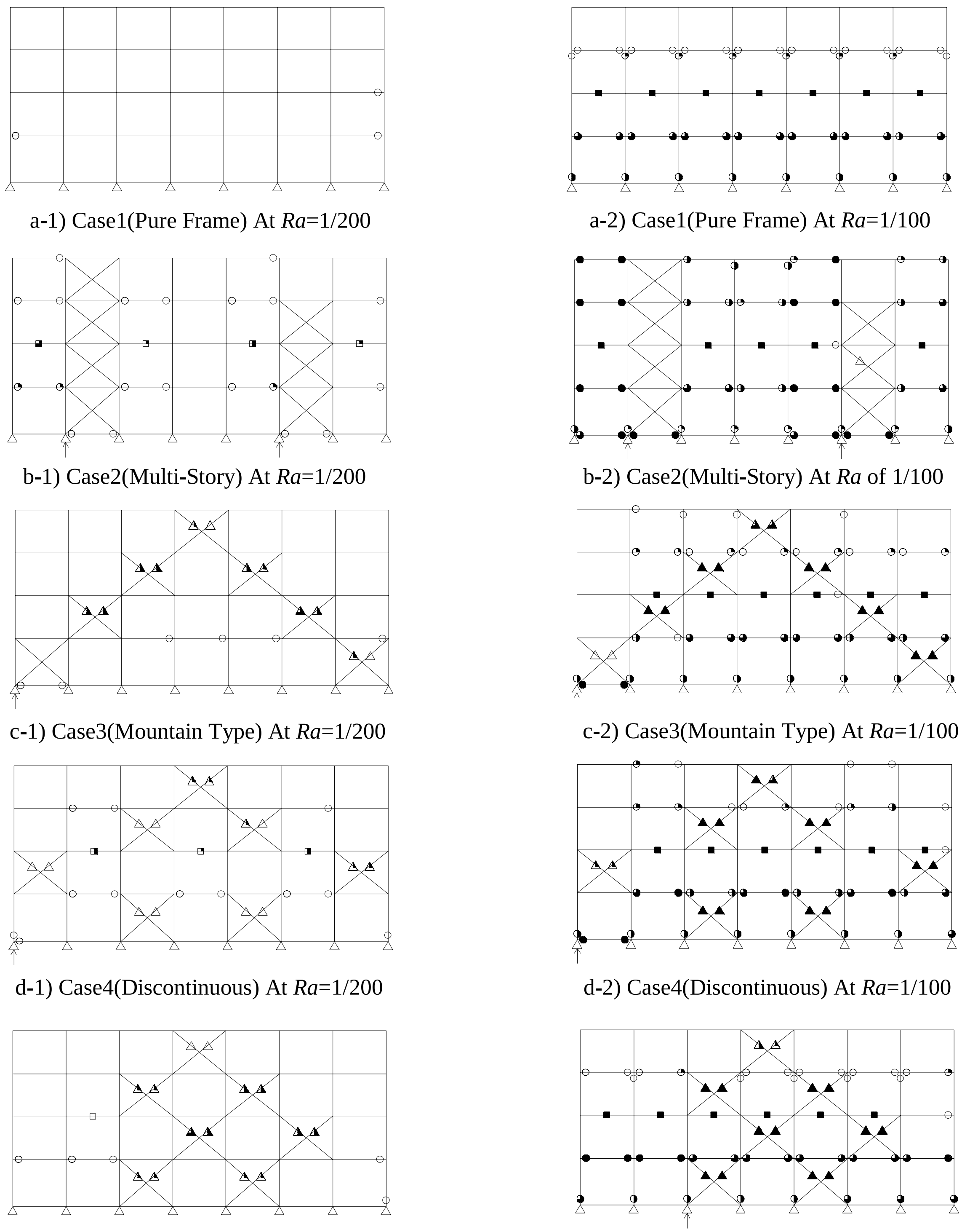

a-1) Case1(Pure Frame) At *Ra*=1/200

a-2) Case1(Pure Frame) At *Ra*=1/100

b-1) Case2(Multi-Story) At *Ra*=1/200

b-2) Case2(Multi-Story) At *Ra* of 1/100

c-1) Case3(Mountain Type) At *Ra*=1/200

c-2) Case3(Mountain Type) At *Ra*=1/100

d-1) Case4(Discontinuous) At *Ra*=1/200

d-2) Case4(Discontinuous) At *Ra*=1/100

e-1) Case5(Checkered Type) At *Ra*=1/200

e-2） Case5(Checkered Type) At *Ra*=1/100

Figure 6 the Occurrence of Yield Hinges at Overall Story Drift Angles *Ra* of 1/200 and 1/100

note: Crush (↓) and Uplift (↑) of Pile foundation was explained by the arrows in the figure

Brace Axial	△	◭	◮	▲	▲
Column and Beam Bending	○	◔	◑	◕	●
Column and Beam Shear	□	◳	◨	◪	■
Ductility factor μ	１．０～１．５	１．５～２．０	２．０～２．５	２．５～３．０	３．０以上

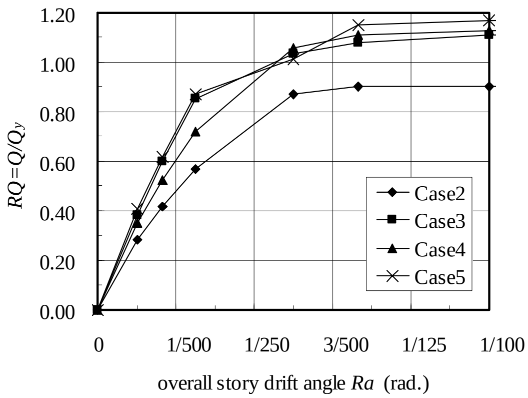

Figure 7 Relationship between RQ at 1st Floor Brace Frame and Ra

Table 4 Shear Force Q_y Occurring at the Failure of the Braces in a Braced Frame

Number of floors	Interior Column	Exterior Colimn	Brace	Brace Frame of Center	Brace Frame of Both Ends
n	$_cQ_u$ (kN)	$_cQ_u$ (kN)	$_sQ_u$ (kN)	Q_y (kN)	Q_y (kN)
4F	838.2	824.9	2017.1	2855.2	2842.0
3F	864.7	838.2	2017.1	2881.7	2855.2
2F	1082.6	1042.8	2514.5	3597.0	3557.3
1F	1102.7	1049.7	2514.5	3617.1	3564.2

Axial force working on columns directly under braced frame

Figure 8 shows the relationship between the ratio RN_c of the axial force N_c acting on the columns on the floor directly under the braced span to the axial force $Q_y \cdot h/L$ acting on the columns on the underlying floor caused by the shear force Q_y occurring at the failure of the bracing in a braced frame, and the overall story drift angle R_a. The graphs of Figure 8 show the results for lower-floor (first-floor) columns that were thought to be on the tension side and the compression side, respectively. In the graphs, axial compressive forces are shown as positive forces, and axial tensile forces as negative forces. The graphs indicate the following:

1) At early stages in all cases (around R=1/1000), long-term axial force acts on the column on the tension side, so the net result is compression of the column. The column on the compression side is acted upon by long-term axial force plus axial force exerted by the bracing, so the net result is large axial compressive force acting on the column.
2) In Case 2 (multi-story), considerably large axial forces act on the first-floor columns, and RN_c at R=1/100 is about −0.7 and 1.4. On the compression side, RN_c=1.0 is considerably exceeded because the lower stories receive greater axial forces.
3) In Case 3 (mountain), Case 4 (discontinuous) and Case 5 (checkered), RN_c values both on the compression side and on the tension side stay within 1.0. This indicates that compared with multi-story continuous bracing, discontinuous bracing has the effect of reducing axial force acting on the columns. Thus, the axial forces acting on the lower-floor columns in the case of discontinuous bracing are smaller than the calculated values of column axial force $Q_y \cdot h/L$ determined by the load-carrying capacity Q_y of the braced frame.

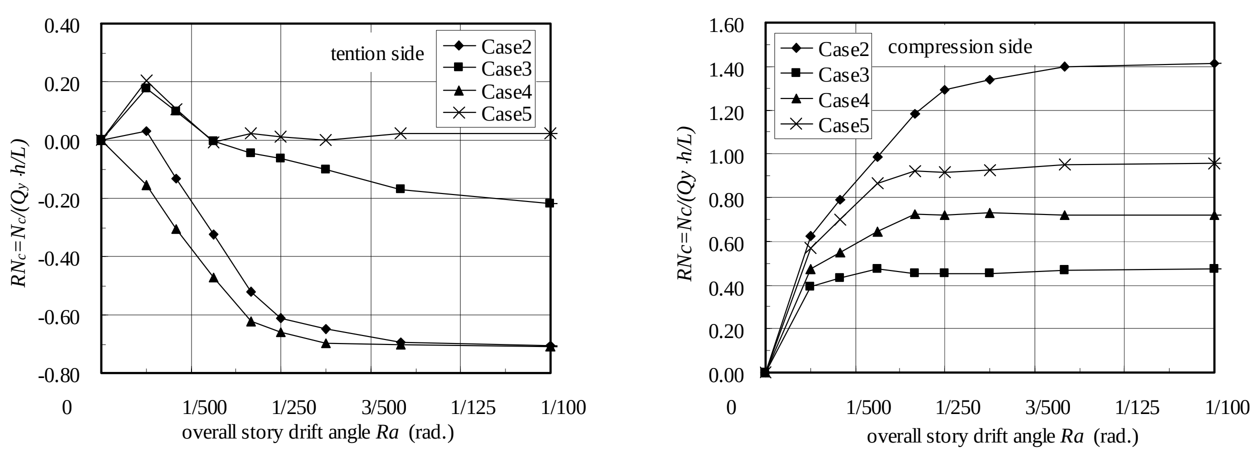

Figure 8 Relationship between RN_c and Ra

note: $RN_c=N_c/(Q_y \cdot h/L)$, Q_y calls at Table 4, h: story height, L: span length

Axial forces acting on adjoining beams

Figure 9 shows the relationship between the ratio RN_g of the axial force N_g acting on the beams adjoining to the braced frame to the shear force Q_y occurring at the failure of the brace frame, and the overall story drift angle R_a. The figure shows the values for the beams at the second and fourth floor levels on the left side of the braced frame. In the graphs, axial compressive forces are shown as positive forces, and axial tensile forces as negative forces. The graphs indicate the following:

1) In Case 2 (multi-story), the RN_g values are small, and axial forces acting on the beams are not very large. In Case 4 (discontinuous), RN_g values are as large as about 0.50. This indicates that in the case of discontinuous bracing, a high percentage of the shear force Q_y acting on the braced frame is transferred in the form of beam axial force.
2) In Case 5 (checkered), RN_g values are close to those in Case 2 (multi-story) and somewhat small (around 0.2) although checkered bracing is a type of discontinuous bracing. The reason for this is thought to be that in the case of checkered bracing, braces were provided in only four spans, as compared with seven spans in Case 3 (mountain) and Case 4 (discontinuous). Because the number of braced spans in Case 4 was closer to that (two spans) in Case 2 (multi-story), the effect of continuous span bracing became relatively great.
3) In none of the cases considered, RN_g values are not greater than about 0.5; so axial forces are about 50% of the load-carrying capacity Q_y of the braced frame. In the case of discontinuous bracing, therefore, the peak value of beam axial force due to Q_y is thought to be around $Q_y/2$.

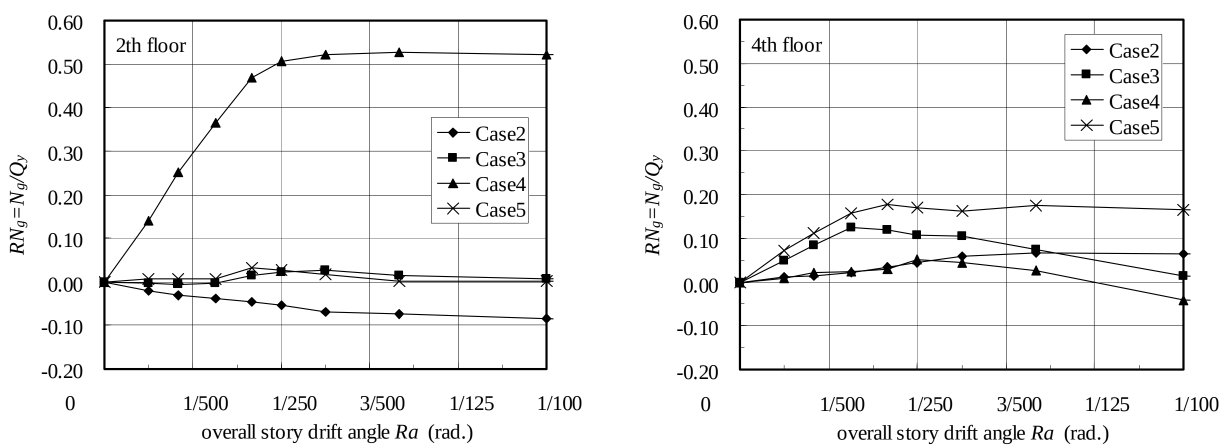

Figure 9 Relationship between RN_g and Ra

note: $RN_g=N_g/Q_y$

Uplift and compression of the foundation

Figure 10 shows the relationship between the ductility factor μ_f for vertical springs that allow for the uplift and compression of the foundation and the overall story drift angle R_a. In general, foundations tend to be less resistant to uplift force than to compressive force. As shown in Table 2, the tension (uplift) capacity of the vertical spring used in the analysis is smaller than its compression capacity. Figure 10, therefore, shows the μ_f –R_a relationship for an internal column foundation that is thought to undergo uplift instead of compression. Figure 10 indicates the following:

1) The ductility factor μ_f at R_a=1/200 in Case 2 (multi-story continuous) is 2.91, which is higher than in any other case because four-story continuous bracing is provided. The next highest values of the ductility factor are 0.77 and 0.95 occurring in Case 4 (discontinuous) and Case 5 (checkered), in both of which braces are provided at two levels (in the X3). In Case 3, too, braces are provided at two levels (in the X3), but μ_f is as small as 0.25 because the tensile force acting on the third-floor column is canceled out by the compressive force acting on the second-floor column.

2) In Case 4 (checkered), the degree of increase in the ductility factor due to increasing deformation is lower than that in Case 2 (multi-story continuous), but μ_f exceeds 1.0 at R_a=1/200.

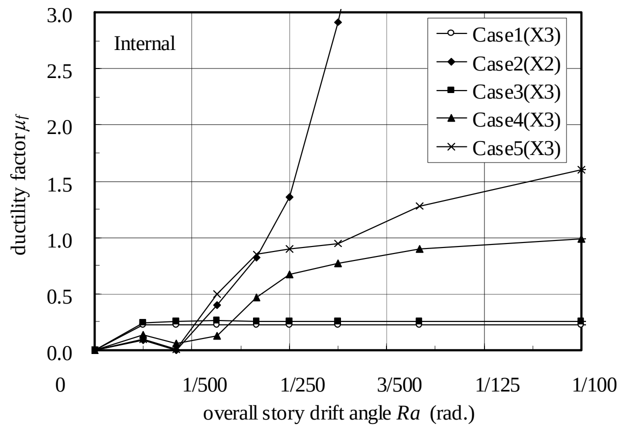

Figure 10 Relationship between of μ_f and Ra (internal column foundation)

SIMPLE EVALUATION METHOD AND THE CONDITIONS FOR ITS APPLICATION

The analysis in the preceding section has shown that in the case of multi-story continuous bracing, increases in column axial force due to the frame-base bending moment result in a rotational mode of failure so that the shear capacity of upper-floor braces decreases or even reverse shear results. If the earthquake resistance of an intermediate story of a building is particularly low and multi-story continuous bracing is provided from the lowest story to the low-earthquake-resistance story of the building, then the shear capacity of that story usually decreases and obviously the other stories become excessively strong. If braces are arranged in a discontinuous manner and the adjacent columns and beams are able to withstand axial forces and transfer shear forces, the braces can provide yield strength to increase the load-carrying capacity and overall stiffness of the building.

From these results, a number of considerations in designing discontinuous bracing have been identified:

(1) As described in Reference 7, the horizontal load-carrying capacity of a braced frame should be calculated taking into account the flow of forces in the existing reinforced concrete and steel frames and brace connections. Because the purpose of discontinuous bracing is to induce yielding of bracing, the bracing system should be designed so that the bracing yields first.

(2) Another important consideration is the performance of the columns on the underlying floor. In cases where the bracing system used is not multi-story continuous type, an unbraced frame underlying a braced frame becomes vulnerable to collapse if the columns at the unbraced floor level are unable to withstand axial forces. The retrofit system, therefore, should be designed so that the columns on the underlying floor can withstand tension and compression until the bracing members of the braced frame yield. Axial forces acting on the columns are caused by global bending occurring at the failure of the bracing members of the braced frame, but the axial force level for the yielding of bracing should be set at a lower level, allowing for the springback (confining effect) of the bent boundary beams.

Equation (1) is compared with Eq. (2) and Eq. (3) to confirm that ${}_cN_y$ does not exceed ${}_cN_T$ or ${}_cN_c$. The ultimate strength and the mode of failure of the lower-floor columns are determined by using the axial force values determined by adding up the ${}_cN_y$ values. If the overlying story is also braced, the values of ${}_cN_y$ due to the upper-floor bracing are added, too.

$$ {}_cN_y = \frac{{}_sQ_y \cdot h - \sum M_g}{L} \quad (1) $$

$$ {}_cN_T = {}_cN_0 + T \quad (2) $$

$$ T = {}_ca_g \cdot \sigma_y $$

$$ {}_cN_c = C - {}_cN_0 \quad (3) $$

$$ C = 0.4b_c \cdot D_c \cdot \sigma_B \ (x > 100mm) $$
$$ C = 0.5b_c \cdot D_c \cdot \sigma_B \ (x \leq 100mm) $$

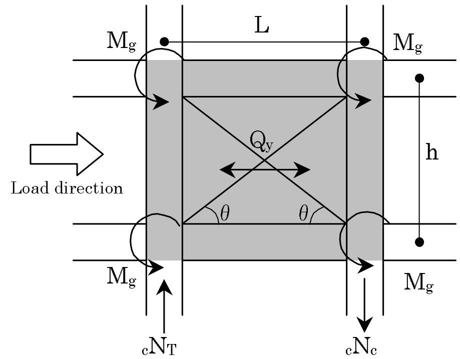

where
${}_cN_y$: axial force acting on column at failure of bracing
${}_sQ_y$: load-carrying capacity of braced frame
h: story height, L: span length
ΣM_g: confining effect of boundary beam
${}_cN_T$: tensile axial force acting on column
${}_cN_0$: long-term axial force acting on column
T: tension capacity
${}_ca_g$: total cross-sectional area of main column reinforcement
σ_y: yield strength of main reinforcement
${}_cN_c$: compressive axial force acting on column
C: compression capacity of column
b_c: column width
D_c: column depth
σ_B: compressive strength of concrete
x: hoop spacing

(3) As a yet another consideration, it is necessary to determine whether or not the shear force carried by the upper-story braced frame can be transferred to the underlying story. In the case of discontinuous bracing, it is difficult to have the two columns on the underlying floor carry the shear forces from a braced frame because of relative weakness of the underlying wall (frame). In reality, however, shear forces are transferred to the lower-floor columns and walls through the beams and floor slabs, so checks are made to make sure that the shear force carried by the braced frame is indeed transferred in the form of axial forces in the beams. It is necessary, therefore, to determine whether or not the shear force occurring at the failure of the braces in the braced frame can be transferred to the adjoining frames. The amount of axial force acting on the beams is calculated assuming that the tension side beam and the compression side beam carry 1/2 of the axial force at the failure of bracing, respectively, and taking into account the forces transferred through the floor slabs. In the analysis of tensile axial forces acting on the beams, forces in the midspan region, where the cross-sectional area of main reinforcement is relatively small, are examined.

Equation (4) is compared with Eq. (5) and Eq. (6) to confirm that ${}_gN_y$ does not exceed ${}_gN_T$ or ${}_gN_c$. The ultimate strength and the mode of failure of the adjoining beams are determined by using the values of the axial force due to this ${}_gN_y$.

$$ {}_g N_y = \frac{{}_s Q_y}{2} - (Q_c + N_s) \qquad (4) $$

$$ N_s = 0.1 t_s \cdot l_s \cdot \sigma_B + a_{st} \cdot \sigma_{sy} $$

$$ {}_g N_T = {}_g a_g \cdot \sigma_y \qquad (5) $$

$$ {}_g N_c = 0.4 b_g \cdot D_g \cdot \sigma_B \qquad (6) $$

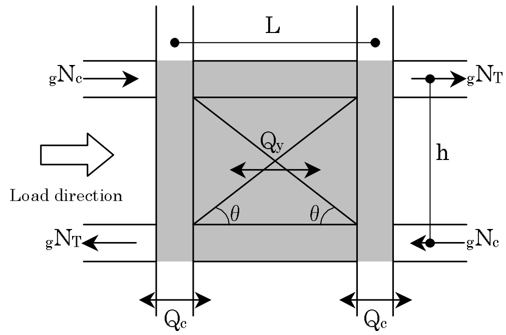

where
${}_gN_y$: axial force acting on beam at failure of bracing
Q_c: ultimate strength of the columns on the underlying floor
N_s: axial force carried by floor slab
t_s: slab thickness
l_s: effective width of slab (assumed to be 1.0 m for simplification)
a_{st}: total cross-sectional area of slab reinforcement
σ_{sy}: yield strength of slab reinforcement
${}_gN_T$: tensile axial force acting on beam
${}_ga_g$: total cross-sectional area of main beam reinforcement
${}_gN_c$: compressive axial force acting on beam
b_g: beam width
D_g: beam depth

(4) The next considerations are the uplift and compression of the foundation. In order to induce yielding of the braces in a braced frame, it is necessary to prevent the rotation of the foundation due to uplift or compression. Vertical axial forces, therefore, acting on the foundation (first floor) are analyzed to confirm that the uplift capacity ${}_fN_T$ and the compression capacity ${}_fN_c$ of the foundation are greater than axial force acting on the foundation.

$$ {}_f N_T = {}_c N_0 + W_1 + W_f + (R) \qquad (7) $$

$$ {}_f N_c = B_s - {}_c N_0 - W_1 - W_f \qquad (8) $$

where
${}_fN_T$: uplift capacity of foundation
W_1: weight of first floor
W_f: self-weight of foundation
R: pull-out capacity of pile
${}_fN_c$: compression capacity of foundation
B_s: bearing capacity of ground or pile

These analyses make it possible to control the mode of failure so that the bracing members in braced frames yield first and to arrange bracing members in a discontinuous manner. Since, however, there are still many unknowns such as the effect of orthogonality in the case of discontinuous bracing and energy absorption capacity under cyclic loading or earthquake loading, it is desirable in static evaluation that the following conditions be satisfied:

1) In cases where strengthening members are arranged in a discontinuous manner, the number of brace locations within a single span (i.e., at multiple floor levels) should not exceed three or four. Too many

braces will result in the occurrence of large axial forces acting on the columns at the lowest floor level and of foundation rotation so that the braces are rendered ineffective.

2) In the case of multi-story buildings with transverse shear walls, such as school buildings and multi-unit dwellings, the contribution of transverse walls can be expected.
3) Since the mode of failure due to yielding of braces is assumed, there is a limit to the level of braced frame strength that can be achieved and to the size of braces that can be used. Exact limits can only be determined through calculation based on the performance of adjoining members, but the rule of thumb is not to use H-beams larger than "H-200×200×8×12" (flange width × web width × flange thickness × web thickness; cross-sectional area: 6,353 mm^2) beams.
4) When parameters such as the stiffness ratio and the modulus of eccentricity are calculated, not only the stiffness and weight of braced frames but also those of secondary walls (e.g., wing walls, inset walls) should be evaluated appropriately. Stiffness and weight distribution should not be made discontinuous; instead, it should be made uniform.

CONCLUSIONS

This paper has proposed a seismic retrofit method using discontinuous bracing, as a non-multi-story continuous bracing approach, and has described a static evaluation method to be used in combination with the retrofit method. The proposed retrofit method is thought to be useful for the seismic retrofit of middle- and high-rise buildings to which the multi-story continuous bracing approach cannot be applied [10]. This paper has also described conditions for using the discontinuous bracing method of seismic retrofit.

REFERENCES

1. S. TANI , S. OGISHI, “Arrangement of Bracings in Frame and Its Effect on Stiffness” , TRANSACTION OF THE ARCHITECTURAL INSTITUTE OF JAPAN No.53, pp50~55, 1956
2. S. TANI, K. HORIKOSHI, “Arrangement of Bracings in Frame and Its Effect on Stiffness (2) (3)”, TRANSACTION OF THE ARCHITECTURAL INSTITUTE OF JAPAN No.57, pp421~428, 1957
3. Y. SONOBE , M. YOKOYAMA , H. IMAI , K. KOSUGI, “RESEARC ON FAILURE MECHANISMS OF FRAMES WITH SHEAR WALLS (EXPERIMENTS ON TWO FRAMES OF DIFFERING SHEAR WALL ARRANGEMENTS)”, TRANSACTION OF THE ARCHITECTURAL INSTITUTE OF JAPAN No.272, pp21~29, 1978
4. AIJ (Architectural Institute of Japan), “AIJ Standard for Structural Calculation of Reinforced Concrete Structures”, 1996
5. JBDPA (The Japan Building Disaster Prevention Association), “Standard for Evaluation of Seismic Capacity of Existing Reinforced Concrete Buildings (2001 Revised Edition), 2001
6. AIJ, “Data for Ultimate Strength Design of Reinforced Concrete Structures,” 1991
7. JBDPA, “Guideline for Seismic Retrofitting Design of Existing Reinforced Concrete Buildings (2001 Revised Edition)”, 2001
8. AIJ, “Recommendations for Design of Building Foundations”, 1996
9. PBA (Public Buildings Association), “Design Standard for Building Structure-1998 Edition, 1998
10. T. KOMURO, M. HIROSAWA, “STUDY ON SEISMIC RETROFIT EFFECT WITH CONTINUOUS AND DISCONTINUOUS ARRANGEMENT OF SEISMIC ELEMENTS”, Proceeding of the Japan Concrete Institute Vol.24 No.2, pp1237~1242, 2002